RSC Advances

ROYAL SOCIETY OF CHEMISTRY

www.rsc.org/advances

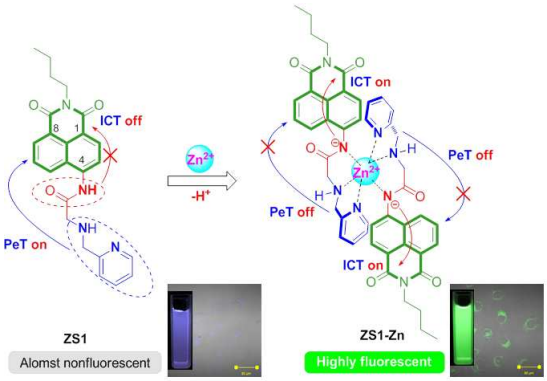

Cite this: DOI: 10.1039/c0xx00000x

www.rsc.org/xxxxxx

ARTICLE TYPE

Combining PeT and ICT Mechanism into One Chemosensor for the Highly Sensitive and Selective Detection of Zinc

Ting Wei, Jinglu Wang, Yu Chen, Yifeng Han*

Received (in XXX, XXX) Xth XXXXXXXXX 20XX, Accepted Xth XXXXXXXXX 20XX

DOI: 10.1039/b000000x

A novel fluorescent sensor (**ZS1**) based on dual-mechanism of PeT/ICT for the highly sensitive and selective detection of Zn^{2+} was designed and synthesized. **ZS1** displays remarkable selectivity for Zn^{2+} with an enhanced red-shift in both absorption and emission resulting from the Zn^{2+}-triggered deprotonation of amide group. **ZS1** could detect as low as 7.2×10^{-9} M Zn^{2+} with an association constant value of 6.27×10^{4} M^{-1}. More importantly, it displayed specific and sensitive recognition to Zn^{2+} and especially avoided the interference of Cd^{2+} in aqueous solution. The probe is also demonstrated to detect Zn^{2+} in living cells.

Introduction

Zinc, widely distributed in the air, water, and solid, is the second most abundant transition metal ions in organisms.[1] Zinc plays crucial roles in many important biological processes such as the structural and catalytic cofactors, neural signal transmitters, and gene expression regulators. The normal concentration range for zinc ions in biological systems is narrow, with both deficiencies and excesses causing many pathological states, such as Alzheimer's disease (AD), amyotrophic lateral sclerosis (ALS), epilepsy, Parkinson's disease, ischemic stroke, and infantile diarrhea.[2] Accordingly, it is desirable to develop new analytical methods for detecting and monitoring zinc ions in vitro and in vivo.

In fact, numerous fluorescent sensors have been developed to detect and analyze zinc ions for its simplicity, high sensitivity, and real-time detection.[3] Unfortunately, only few zinc ion fluorescent sensors that can distinguish Zn^{2+} from Cd^{2+} with high selectivity have been reported.[4] Zn^{2+} and Cd^{2+} are in the same group of periodic table and have similar properties which will cause similar spectral changes while coordinated with fluorescent sensors. Therefore, for practical applications, it is still strongly desirable to develop fluorescent chemosensors with excellent performance for Zn^{2+} under physiological conditions.

It should be noted that compared with conventional one mechanism such as photo-induced electron transfer (PeT),[5] excited-state intramolecular proton transfer (ESIPT),[6] intramolecular charge transfer (ICT),[7] and aggregation-induced emission (AIE)[8] based sensors which usually give one single signaling response, the combination of two or more mechanisms based sensors would be more attractive since such a multi-mechanism will usually produce multiple signals to amplify recognition events to a greater extent and finally improve selectivity and sensitivity. To date, several fluorescent sensors have been developed on the basis of multi-mechanism. For example, Akkaya et al. reported BODIPY-derived probes to sensing of Hg^{2+}, GSH, and biological thiols based on PeT/ICT dual-mechanism.[9] Wang and Zhang et al. applied PeT/ESIPT dual-mechanism to design a 3-hydroxyflavone based probe for thiols.[10] However, the combination of PeT/ICT dual-mechanism based zinc sensors have scarcely explored. Recently, Yoon, Shin, and Xu et al. developed a novel PeT/ICT dual-mechanism based fluorescent sensor by Zn^{2+}-triggered amide tautomerization for highly selectivity of zinc,[4a] which is difficult to accomplish via a single mechanism.

Inspired by all of these works, we report here a novel PeT/ICT dual-mechanism based fluorescence turn-on zinc sensor **ZS1**, 2-picolylamine (PA) derivative of 4-aminonaphthalimide, for the detection of Zn^{2+}. In **ZS1**, an amide group has been inserted to link the 1, 8-naphthalimide fluorophore and PA chelator. We envisioned that the fluorescence of **ZS1** would be quenched by PeT effect from PA chelator but also by ICT effect from 4-amide

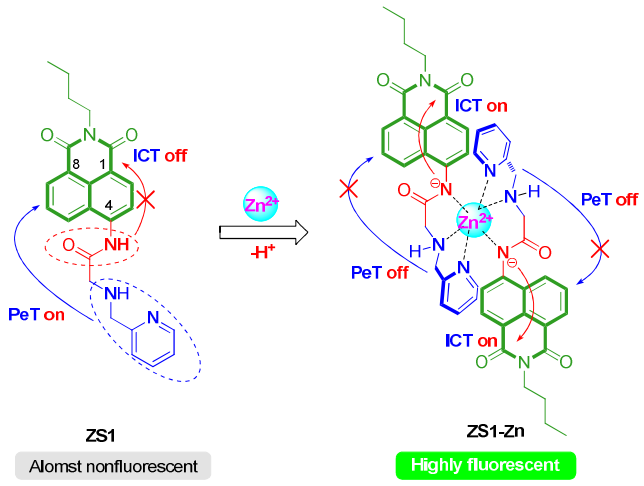

Scheme 1 The PeT/ICT dual-mechanism response strategy for the design of **ZS1**.

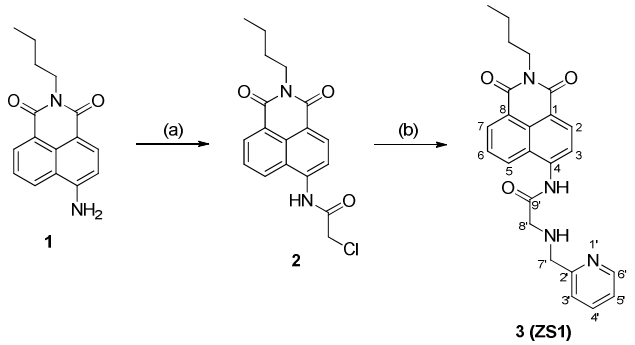

Scheme 2 Synthesis of **ZS1**: (a) 2-chloroacetyl chloride/NEt_3, DCM, reflux, 1h, 89%; (b) 2-picolylamine/DIPEA/KI, CH_3CN, reflux, 10h, 48%.

group. However, the capture of Zn^{2+} by the amide-PA receptor resulted in red shifts in both absorption and fluorescence spectra due to the repressed PeT process from the N atoms of PA to the fluorophore and the enhanced ICT process from N atom in 4 position of **ZS1** to the 1, 8-naphthalimide by the deprotonation of the NH in 4-amide group. This kind of binary effects of PeT/ICT mechanisms of Zn^{2+} to **ZS1** exhibits high binding affinity and selectivity towards Zn^{2+} (Scheme 1).

Results and discussion

ZS1 can be readily prepared in two convenient steps under facile reaction conditions with high yield starting with 4-amino-*N*-butyl-1, 8-naphthalimide (**1**). The product (**ZS1**) was well characterized by ^1H, ^{13}C NMR, and HR-MS (Scheme 2).

In the UV-vis absorption spectra (Fig. 1), **ZS1** exhibits a broad band from 300 to 450 nm with its maximum centered at 360 nm, which is assigned to the π-π* transitions of the 1, 8-naphthalimide. Upon addition of Zn^{2+} (0-10.0 equiv.), this band red-shifts to 366 nm, accompanying three clear isosbestic points at 266, 342, and 407 nm, respectively, which was due to the deprotonation of amide NH group and this deprotonation process strengthens the electron-donating ability from the nitrogen atom of 4-amide group to the 1,8-naphthalimide. Furthermore, a good linear relationship (R^2 = 0.994) was observed between the changes in the absorbance at 366 nm with Zn^{2+} in the range of 0-120.0 μM (Fig. S1, ESI†).

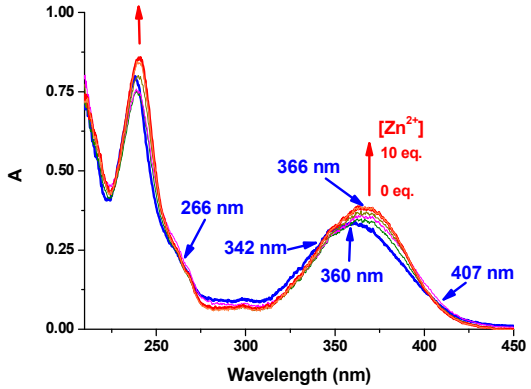

Fig. 1 Absorption spectra of **ZS1** (20.0 μM) in Tirs-HCl buffer (10 mM, pH 7.2, containing 1% CH_3CN) in the presence of different concentrations of Zn^{2+} (0-10.0 equiv.).

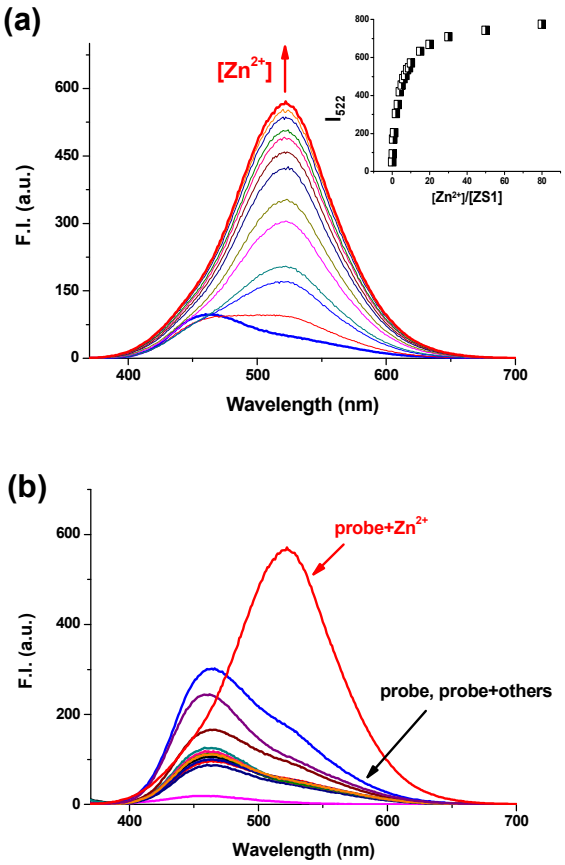

Fig. 2 (a) Fluorescence spectra of **ZS1** (10.0 μM) in Tirs-HCl buffer (10 mM, pH 7.2, containing 1% CH_3CN) in the presence of different concentrations of Zn^{2+} (0-80.0 equiv.) (λ_{ex} = 360 nm). Inset: fluorescence intensity (λ_{em} = 522 nm) changes as a function of Zn^{2+} concentration. (b) Emission spectra of **ZS1** (10.0 μM) in Tirs-HCl buffer (10 mM, pH 7.2, containing 1% CH_3CN) in the presence of various metal ions (λ_{ex} = 360 nm, 10.0 eq. of Ag^+, Ca^{2+}, Cd^{2+}, Cr^{3+}, Cu^{2+}, Fe^{2+}, Fe^{3+}, Hg^{2+}, K^+, Mg^{2+}, Mn^{2+}, Na^+, Pb^{2+}, and Zn^{2+}, respectively).

As expected, **ZS1** alone is weak blue fluorescence (ε = 11598 $M^{-1}cm^{-1}$, Φ_0 = 0.033, λ_{ex} = 360 nm, λ_{em} = 465 nm, Table S1, ESI†) in neutral aqueous solution (10 mM Tirs-HCl buffer, pH 7.2, containing 1% CH_3CN). While addition of 10.0 equiv. of Zn^{2+} induced a red-shift in the emission of **ZS1** to 522 nm and triggered a *ca*. 5.3-fold (green fluorescence, ε = 12145 $M^{-1}cm^{-1}$, Φ_0 = 0.175, λ_{ex} = 360 nm, λ_{em} = 522 nm, Table S1, ESI†) increase in integrated emission for **ZS1** (Fig. 2a). These fluorescence behaviors were attributed to the coordination of the PA chelator and the deprotonated amide nitrogen of **ZS1** with Zn^{2+} which repressed the PeT effect from PA chelator and enhanced the ICT process from the deprotonated 4-amide group, simultaneously. Titration of **ZS1** with Zn^{2+} was followed by fluorescence to determine the **ZS1**/Zn^{2+} binding ratio and association constant (K_a). K_a of **ZS1**/Zn^{2+} was determined to be 6.27×10^4 M^{-1} by a Hill plot analysis (Fig. 3a). Moreover, a Job's plot, which exhibits a maximum at 0.34 M fraction of Zn^{2+}, indicated that a 2:1 complex is formed between **ZS1** and Zn^{2+} (Fig. 3b). We also carried out the HPLC-MS measurements for the **ZS1**-Zn^{2+} solution (Fig. S3, ESI†). All those results agree well with the proposed structure of the **ZS1**-Zn^{2+} complex (Fig. S4, ESI†).

To clarify the actual **ZS1**/Zn^{2+} interaction, ^1H NMR titration

Cite this: DOI: 10.1039/c0xx00000x

www.rsc.org/xxxxxx

ARTICLE TYPE

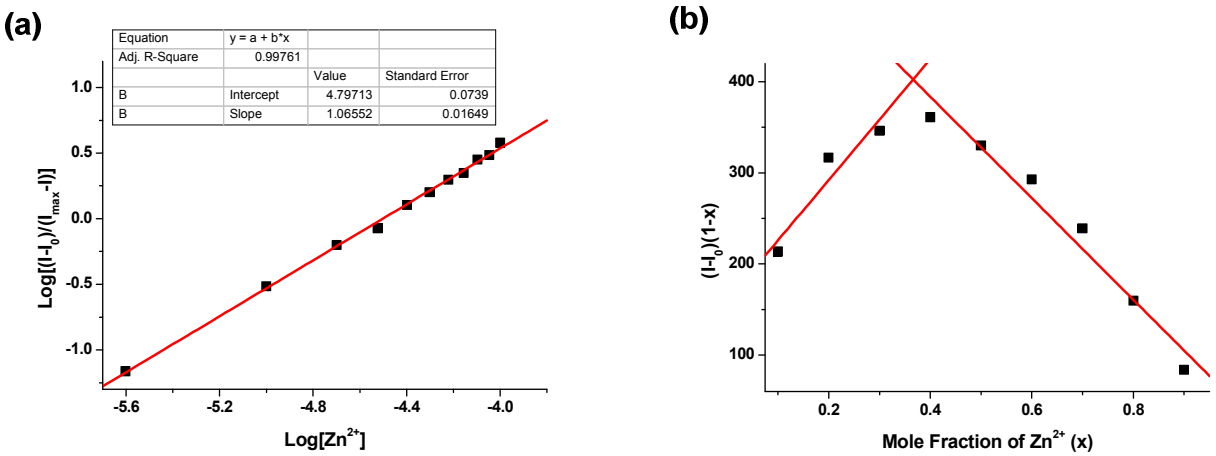

Fig. 3 (a) Hill plot of sensor **ZS1**. Fluorescence intensity at 522 nm responses as a function of Zn^{2+} concentration (10 mM Tirs-HCl buffer, pH 7.2, containing 1% CH_3CN, λ_{ex} = 360 nm). The solid line represents a linear fit to the experimental data. (b) Job's plot of sensor **ZS1**, the total concentration of the sensor and Zn^{2+} is 100.0 μM (10 mM Tirs-HCl buffer, pH 7.2, containing 1% CH_3CN, λ_{ex} = 360 nm).

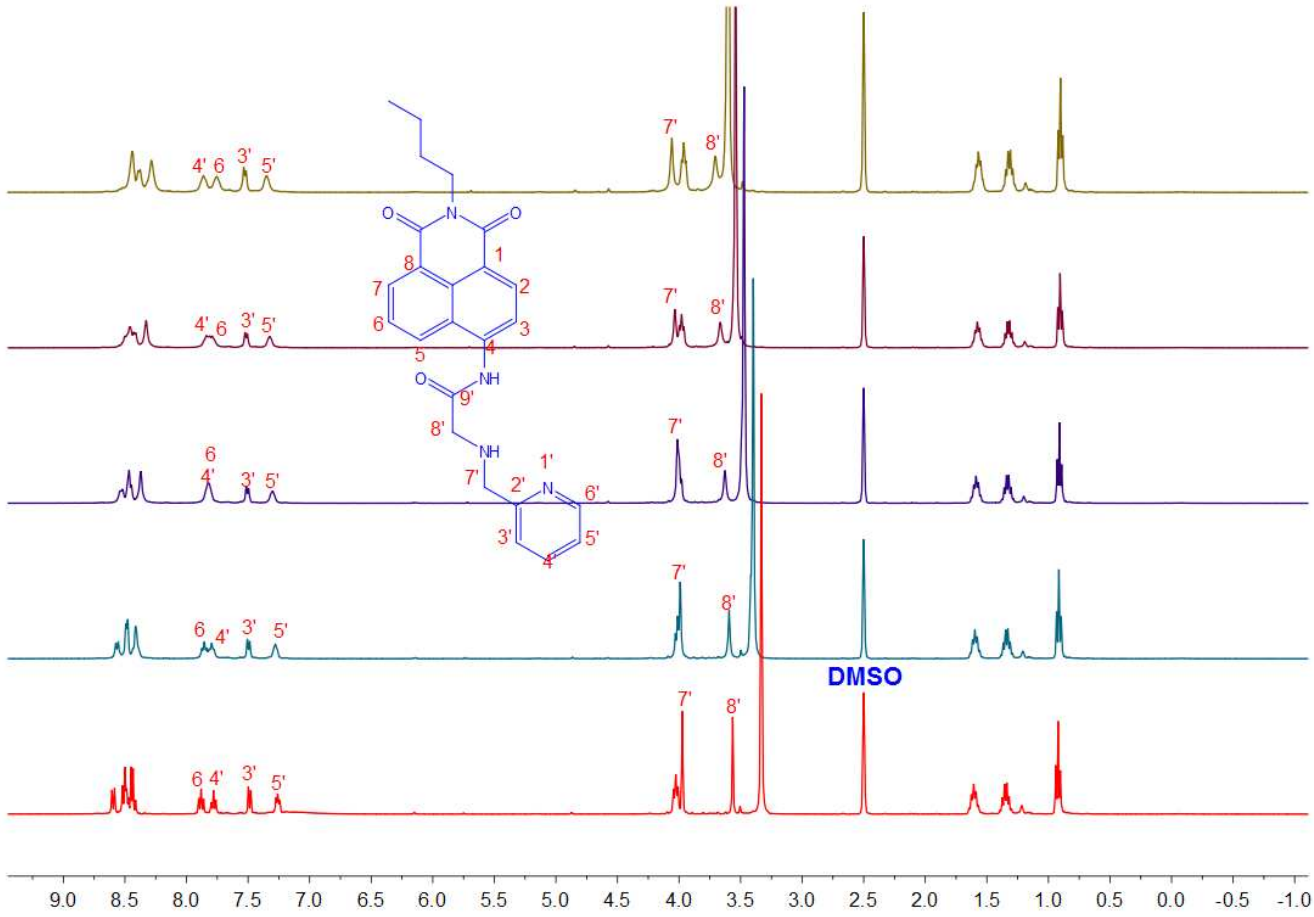

Fig. 4 ^{1}H NMR titration experiment of **ZS1** in the presence of different concentrations of Zn^{2+} (0-10.0 equiv. of Zn^{2+}, in d_6-DMSO).

Cite this: DOI: 10.1039/c0xx00000x

www.rsc.org/xxxxxx

ARTICLE TYPE

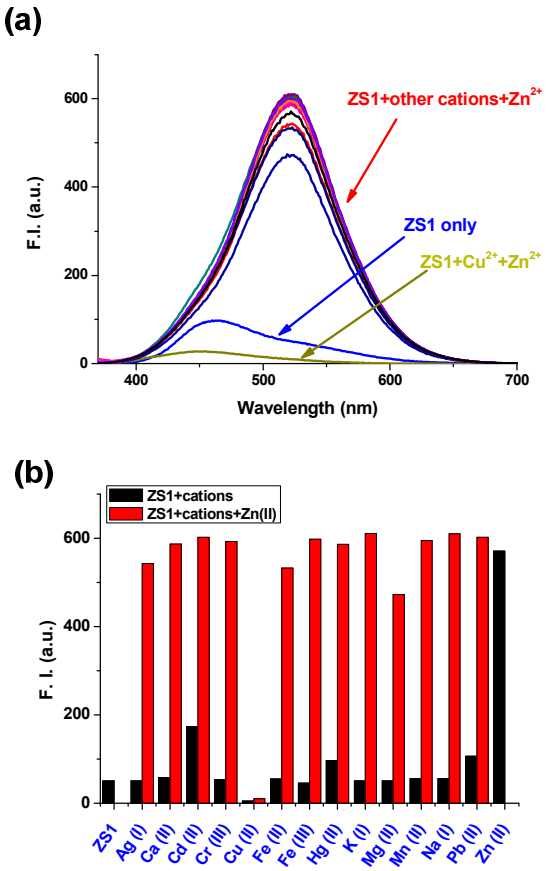

Fig. 5 (a) The fluorescence responses of **ZS1** (10.0 μM) with 10.0 equiv. of the competing metal ions in 10 mM Tirs-HCl buffer, pH 7.2, containing 1% CH_3CN, followed by 10 equiv. of Zn^{2+}, Metal ions include Ag^{+}, Ca^{2+}, Cd^{2+}, Cr^{3+}, Cu^{2+}, Fe^{2+}, Fe^{3+}, Hg^{2+}, K^{+}, Mg^{2+}, Mn^{2+}, Na^{+}, and Pb^{2+}, respectively, λ_{ex} = 360 nm. (b) Fluorescence responses of **ZS1** to various metal ions. Black bars represent the addition of 10.0 equiv. of the appropriate metal ion to a 10.0 μM solution of **ZS1** in 10 mM Tirs-HCl buffer, pH 7.2, containing 1% CH_3CN, λ_{ex} = 360 nm; Red bars represent the addition of 10 equiv. of Zn^{2+} to the solutions containing **ZS1** (10.0 μM, in 10 mM Tirs-HCl buffer, pH 7.2, containing 1% CH_3CN) and the appropriated metals (10.0 equiv.), λ_{ex} = 360 nm.

experiment was conducted. As shown in Fig. 4, the two methylene protons at 3.97 and 3.56 ppm attributed to the H-7′ and 8′, respectively, together with the pyridine protons (H-3′, 4′, 5′, 6′) were dramatically shifted downfield after the addition of Zn^{2+} due to the chelation of the lone-pair electrons of two nitrogen atoms of PA by Zn^{2+}. Meanwhile, the chemical shifts of five aromatic resonances attributed to the 1, 8-naphthalimide protons experienced an opposite shift, indicating that the deprotonation of 4-amide group of **ZS1** has occurred in the presence of Zn^{2+}. Those results agree well with the optical responses.

Further, the fluorescence titration of **ZS1** with various metal ions was conducted to examine the selectivity (Fig. 2b). Much to our delight, the examined alkali, alkaline-earth metal ions, and

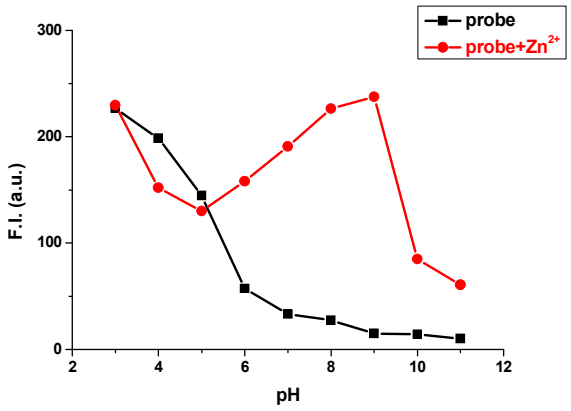

Fig. 6 Effect of the pH on the fluorescence emission of **ZS1** (10.0 μM) alone and **ZS1**-Zn^{2+} system (10.0 μM of **ZS1** in the presence of 10.0 equiv. of Zn^{2+}), slit = 1.5/3.

transition metal ions showed nominal changes in the fluorescence of spectra of **ZS1**. The competing experiments were then tested in the presence of Zn^{2+} mixed with other competing metal ions(Fig. 5a and 5b). Except for Cu^{2+}, other background metal ions had no obvious interference with the detection of Zn^{2+} ions. It should be noted that **ZS1** has displayed a considerable ability to distinguish Zn^{2+} from Cd^{2+}, which have similar properties to Zn^{2+} and generally cause a strong interference.

pH effects on the fluorescence of **ZS1** and the **ZS1**-Zn^{2+} system were also investigated. As depicted in Fig. 6, **ZS1** alone is inert to pH in the range of 12.0-6.0, but the fluorescent intensity dramatically increased from pH 6.0 to 3.0 due to the inhibited PeT process by protonation of the two nitrogen atoms of PA chelator. However, satisfactory Zn^{2+}-sensing abilities were exhibited in a range of pH from 6.0 to 9.0, indicating that **ZS1** could be used in neutral natural systems, or a mildly acidic or basic environment.

For practical purposes, the detection limit of **ZS1** for the analysis of Zn^{2+} was also an important parameter. The fluorescence titration curve revealed that the fluorescence intensity of **ZS1** at 522 nm increased linearly with the amount of Zn^{2+} in the range of 0-5.0 μM (R^2 = 0.99) (Fig. S2, ESI†). Thus, the detection limit of **ZS1** for Zn^{2+} was calculated to be 7.2×10^{-9} M, which reveals the high sensitivity for the analysis of zinc ions by using the **ZS1**.

Duo to the favorable properties of **ZS1** in vitro, the potential utility of **ZS1** in living cells was studied. HeLa cells were incubated with 5.0 μM of **ZS1** for 0.5 h at 37 °C exhibited weak blue fluorescence (Fig. 7a). The cells were then treated with $ZnCl_2$ (5.0 μM) for 0.5 h at 37 °C and resulted in a dramatic increase of intracellular green fluorescence (Fig. 7d), which indicated that **ZS1** was cell membrane permeable and capable of image of Zn^{2+} in living cells.

Conclusion

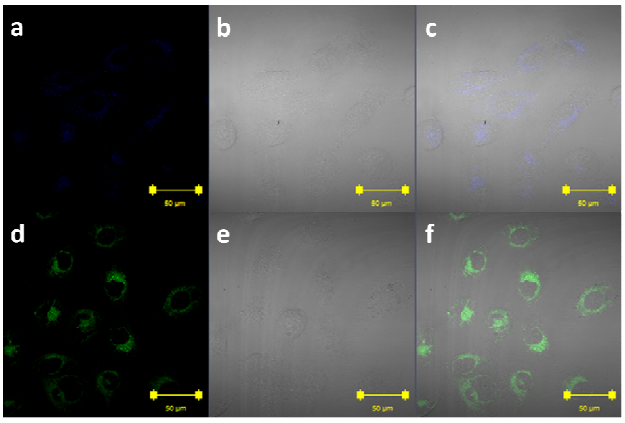

Fig. 7 Fluorescence image of HeLa cells incubated with **ZS1** (5.0 μM) for 0.5 h, and then washed quickly with PBS for imaging (a). (b) Bright-field images of live cells in (a). (c) The overlay images of live cells in (a) and (b). The cells were then treated with $ZnCl_2$ (5.0 μM) for 0.5 h which resulted in a dramatic increase in intracellular green fluorescence (d). (e) Bright-field images of live cells in (d). (f) The overlay images of live cells in (d) and (e).

In conclusion, we have successfully developed a novel PeT/ICT dual-mechanism based fluorescent probe **ZS1** for selective detection of Zn^{2+} in aqueous solution. **ZS1** displays an excellent fluorescent selectivity for Zn^{2+} with an enhanced red-shift in both absorption and emission resulting from the Zn^{2+}-triggered deprotonation of amide group. Moreover, based-on this PeT/ICT dual-mechanism, **ZS1** can easily distinguish Zn^{2+} from Cd^{2+} in aqueous solution, which is usually a technique problem for other related probes. Furthermore, fluorescence imaging of Zn^{2+} in living cells indicated that this probe might be favorable for biological applications. We anticipate that the experimental results of this study will inspire in the future design of metal-ion sensors in water for a variety of chemical and biological applications.

Experimental section

Materials and measurements

All the solvents were of analytic grade. NMR experiments were carried out on a Bruker AV-400 NMR spectrometer with chemical shifts reported in ppm (in $CDCl_3$, d_6-DMSO or TMS as an internal standard). Mass spectrum (MS) was recorded on a SHIMADZU LCMS-2020 spectrometer. All pH measurements were made with a Sartorius basic pH-Meter PB-10. Fluorescence spectra were determined on a PerkinElmer LS55 Fluorescence spectrophotometer. Absorption spectra were determined on a Shimadzu UV 2501(PC)S UV-Visible spectrophotometer. Unless otherwise noted, the excitation and emission widths for **ZS1** were all 3.

Synthesis

4-amino-N-butyl-1, 8-naphthalimide (1): compound **1** was obtained according to published procedure.[11] ^{1}H NMR (400 MHz, $CDCl_3$) δ 8.59 (d, J = 7.2 Hz, 1H), 8.41 (d, J = 8.1 Hz, 1H), 8.11 (d, J = 8.4 Hz, 1H), 7.64 (t, J = 7.9 Hz, 1H), 6.88 (d, J = 8.2 Hz, 1H), 5.00 (s, 2H), 4.16 (t, J = 7.2 Hz, 2H), 1.71 (m, 2H), 1.44 (m, 2H), 0.97 (t, J = 7.3 Hz, 3H).

4-(2-chloroacetyl) amino-N-butyl-1, 8-naphthalimide (2): 4-amino-N-butyl-1, 8-naphthalimide (**1**) (500 mg, 1.9 mmol) was dissolved in dry dichloromethane (30 mL), then triethylamine (0.4 mL, 2.9 mmol) and 2-chloroacethyl chloride (0.2 mL, 2.5 mmol) were added under 0 oC and the solution was refluxed for 1 h until all starting material got consumed which was monitored by TLC analysis. The reaction mixture was washed with water (100 mL), extracted with dichloromethane (3 × 50 mL). The extract was dried over sodium sulfate and then concentrated under vacuum. The product was purified by flash chromatography using petroleum ether/dichloromethane (1:2, v/v) as eluant to give **2** as a pale yellow solid (580 mg, 89%); ^{1}H NMR (400 MHz, $CDCl_3$) δ 9.14 (brs, 1H), 8.64 (m, 2H), 8.48 (d, J = 7.9 Hz, 1H), 8.19 (d, J = 8.4 Hz, 1H), 7.83 (t, J = 7.7 Hz, 1H), 4.40 (s, 2H), 4.18 (t, J = 7.2 Hz, 2H), 1.71 (m, 2H), 1.45 (m, 2H), 0.98 (t, J = 7.1 Hz, 3H).

4-(2-(picolylamino)acetyl)amino-N-butyl-1,8-naphthalimide (3, ZS1): 4-(2-chloroacetyl) amino-N-butyl-1, 8-naphthalimide (**2**) (300 mg, 0.87 mmol), 2-picolylamine (0.17 mL, 1.65 mmol), N,N-diisopropylethylamine (DIPEA) (1.50 mL), and potassium iodide (90 mg) were added to acetonitrile (50 mL). The mixture solution was then refluxed for 10 h until all starting material got consumed which was monitored by TLC analysis. The solvent was then removed under reduced pressure to obtain dark oil, which was purified by flash chromatography using ethyl acetate as eluant to give **3** as a pale yellow solid (173 mg, 48%); R_f = 0.60 (12:1 dichloromethane: methanol); M.p. = 131-132 °C; ^{1}H NMR (400 MHz, $CDCl_3$) δ 10.99 (brs, 1H), 8.68 (d, J = 8.2 Hz, 1H), 8.61 (m, 2H), 8.55 (d, J = 4.7 Hz, 1H), 8.43 (d, J = 8.5 Hz, 1H), 7.75 (t, J = 7.9 Hz, 1H), 7.69 (td, J = 7.7, 1.6 Hz, 1H), 7.27 – 7.18 (m, 2H), 4.17 (t, J = 7.2 Hz, 2H), 4.10 (s, 2H), 3.64 (s, 2H), 1.72 (m, 2H), 1.45 (m, 2H), 0.98 (t, J = 7.3 Hz, 3H); ^{13}C NMR (100 MHz, $CDCl_3$) δ 170.40, 164.25, 163.69, 157.81, 149.73, 138.78, 136.85, 132.67, 131.02, 128.94, 126.53, 123.25, 122.72, 122.52, 118.02, 117.03, 54.99, 53.13, 40.20, 30.22, 20.38, 13.82; HR-MS (ESI-TOF): *m/z* 417.1960 $[M+H]^+$, *calc'd.* 417.1927.

Acknowledgements

This work was supported by the National Natural Science Foundation of China (Grant No. 20902082), the Zhejiang Provincial Natural Science Foundation of China (Grant No. Y3100416) and the Program for Innovative Research Team of Zhejiang Sci-Tech University (13060052-Y).

Notes and references

Department of Chemistry, The Key Laboratory of Advanced Textile Materials and Manufacturing Technology, Zhejiang Sci-Tech University, Hangzhou, 310018, China.
E-mail: zstuchem@gmail.com; Tel: +86-751-86843550

† Electronic Supplementary Information (ESI) available: Experimental details, synthetic details of MS1, additional spectroscopic data, and copies of NMR spectra. See DOI: 10.1039/b000000x/

1 (*a*) P. Jiang and Z. Guo, *Coord. Chem. Rev*., 2004, **248**, 205; (*b*) J. M. Berg and Y. Shi, *Science*, 1996, **271**, 1081; (*c*) X. Xie and T. G. Smart, *Nature*, 1991, **349**, 521; (*d*) B. L. Vallee and K. H. Falchuk, *Physiol. Rev*., 1993, **73**, 79; (e) K. H. Falchuk, Mol. Cell. *Biochem*., 1998, **188**, 41.

2 (*a*) A. I. Bush, *Curr. Opin. Chem. Biol*., 2000, **4**, 184; (*b*) A. I. Bush, *Trends Neurosci*., 2003, **26**, 207; (*c*) M. P. Cuajungco and G. J. Lees, *Brain Res. Rev*., 1997, **23**, 219.

3 (*a*) Z. Guo, S. Park, J. Yoon and I. Shin, *Chem. Soc. Rev*., 2014, **43**, 16; (*b*) Z. Liu, W. He and Z. Guo, *Chem. Soc. Rev*., 2013, **42**, 1568; (*c*) L. Yuan, W. Lin, K. Zheng, L. He and W. Huang, *Chem. Soc. Rev*., 2013, **42**, 622; (*d*) G. Zhang, H. Li, S. Bi, L. Song, Y. Lu, L. Zhang, J. Yu and L. Wang, *Analyst*, 2013, **138**, 6163; (*e*) S. Jiao, L. Peng, K. Li, Y. Xie, M. Ao, X. Wang and X. Yu, *Analyst*, 2013, **138**, 5762; (*f*) P. Li, X. Zhou, R. Huang, L. Yang, X. Tang, W. Dou, Q. Zhao and W. Liu, *Dalton Trans*., 2014, **43**, 706; (*g*) Y. Zhang, X. F. Guo, W. X. Si, L. H. Jia and X. H. Qian, *Org. Lett*., 2008, **10**, 473; (*h*) A. Ajayaghosh, P. Carol and S. Sreejith, *J. Am. Chem. Soc*., 2005, **127**, 14962; (*i*) D. A. Pearce, N. Jotterand, I. S. Carrico and B. Imperiali, *J. Am. Chem. Soc*., 2001, **123**, 5160; (*j*) S. C. Burdette, C. J. Frederickson, W. Bu and S. J. Lippard, *J. Am. Chem. Soc*., 2003, **125**, 1778; (*k*) Z. Xu, X. Liu, J. Pan and D. R. Spring, *Chem. Commun*., 2012, **48**, 4764; (*l*) Y. Ding, Y. Xie, X. Li, J. P. Hill, W. Zhang and W. Zhu, *Chem. Commun*., 2011, **47**, 5431.

4 (*a*) Z. Xu, K.-H. Baek, H. N. Kim, J. Cui, X. Qian, D. R. Spring, I. Shin and J. Yoon, *J. Am. Chem. Soc*., 2010, **132**, 601-610; (*b*) Z. Xu, X. Qian, J. Cui and R. Zhang, *Tetrahedron*, 2006, **62**, 10117-10122; (*c*) L. Xue, C. Liu and H. Jiang, *Org. Lett*., 2009, **11**, 1655-1658; (*d*) Y. Tan, J. Gao, J. Yu, Z. wang, Y. Cui, Y. Yang, G. Qian, *Dalton Trans*., 2013, **42**, 11465-11470; (*e*) P. Li, X. Zhou, R. huang, L. Yang, X. Tang, W. dou, Q. Zhao, W. Liu, *Dalton Trans*., 2014, **43**, 706-713; (*f*) K. Wu, Y. Gao, Z. Yu, F. Yu, J. Jiang, J. Guo and Y. Han, *Anal. Methods*, 2014, **6**, 3560-3563; (*g*) M. Khan, C. R. Goldsmith, Z. Huang, J. Georgiou, T. T. Luyben, J. C. Roder, S. J. Lippard and K. Okamoto, *Proc. Natl. Acad. Sci. USA*., 2014, **111**, 6786-6791; (*h*) T. Mistri, M. Dolai, D. Chakraborty, A. R. Khuda-Bukhsh, K. K. Das and M. Ali, *Org. Biomol. Chem*., 2012, **10**, 2380-2384; (*i*) G. Sivaraman, T. Anand and D. Chellappa, *Analyst*, 2012, **137**, 5881-5884; (*j*) J. F. Zhu, W. H. Chan, A. W.M. Lee, *Tetrahedron Lett*., 2012, **53**, 2001-2004; (*k*) L. Praveen, C. H. Suresh, M. L. P. Reddy and R. Luxmi Varma, *Tetrahedron Lett*., 2011, **52**, 4730-4733; (*l*) B. K. Datta, S. Mukherjee, C. Kar, A. Ramesh and Gopal Das, *Anal. Chem*., 2013, **85**, 8369-8375.

5 (*a*) T. Matsumoto, Y. Urano, T. Shoda, H. Kojima, and T. Nagano, *Org. Lett*., 2007, **9**, 3375; (*b*) L.-Y. Lin, X.-Y. Lin, F. Lin, and K.-T. Wong, *Org. Lett*., 2011, **13**, 2216; (*c*) Y. Gabe, Y. Urano, K. Kikuchi, H. Kojima, and T. Nagano, *J. Am. Chem. Soc*., 2004, **126**, 3357; (*d*) J. Wang and X. Qian, *Chem. Commun*., 2006, 109; (*e*) J. Wang, X. Qian and J. Cui, *J. Org. Chem*., 2006, **71**, 4308; (*f*) J. Wang and X. Qian, *Org. Lett*., 2006, **8**, 3721. (*g*) J. Liu, K. Wu, S. Li, T. Song, Y. Han and X. Li, *Dalton Trans*., 2013, **42**, 3854.

6 (*a*) T. I. Kim, H. J. Kang, G. Han, S. J. Chung and Y. Kim, *Chem. Commun*., 2009, 5895; (*b*) R. Hu, J. A. Feng, D. H. Hu, S. Q. Wang, S. Y. Li, Y. Li and G. Q. Yang, *Angew. Chem., Int. Ed*., 2010, **49**, 4915; (*c*) M. Santra, B. Roy and K. H. Ahn, *Org. Lett*., 2011, **13**, 3422; (*d*) Z. Xu, L. Xu, J. Zhou, Y. Xu, W. Zhu and X. Qian, *Chem. Commun*., 2012, **48**, 10871; (*e*) S. Chen, P. Hou, J. Wang and X. Song, *RSC Adv*., 2012, **2**, 10869; (*f*) M. Kumar, N. Kumar and V. Bhalla, *RSC Adv*., 2013, **3**, 1097.

7 (*a*) D. Srikun, E. W. Miller, D. W. Domaille, and C. J. Chang, *J. Am. Chem. Soc*., 2008, **130**, 4596; (*b*) L. Yuan, W. Lin, J. Song and Y. Yang, *Chem. Commun*., 2011, **47**, 12691; (*c*) F. Yu, P. Li, P. Song, B. Wang, J. Zhao and K. Han, *Chem. Commun*., 2012, **48**, 2852; (*d*) X. Li, S. Zhang, J. Cao, N. Xie, T. Liu, B. Yang, Q. He and Y. Hu, *Chem. Commun*., 2013, **49**, 8656; (*e*) J. Liu, K. Wu, X. Li, Y. Han and M. Xia, *RSC Adv*., 2013, **3**, 8924.

8 (*a*) L. Peng, Z. Zhou, R. Wei, K. Li, P. Song, A. Tong, *Dyes and Pigments*, 2014, **108**, 24; (*b*) X. Li, C. Yang, K. Wu, Y. Hu, Y. Han and S. H. Liang, *Theranostics*, 2014, **4**, 1233; (*c*) H. Wang, Y. Huang, X. Zhao, W. Gong, Y. Wang and Y. Cheng, *Chem. Commun*., 2014, **50**, 15075; (*d*) G. N. Zhao, B. Tang, Y. Q. Dong, W. H. Xie and B. Z. Tang, *J. Mater. Chem. B*, 2014, **2**, 5093; (*e*) R. T. K. Kwok, C. W. T. Leung, J. W. Y. Lam and B. Z. Tang, *Chem. Soc. Rev*., 2015, DOI: 10.1039/C4CS00325J.

9 (*a*) O. A. Bozdemir, R. Guliyev, O. Buyukcakir, S. Selcuk, S. Kolemen, G. Gulseren, T. Nalbantoglu, H. Boyaci and E. U. Akkaya, *J. Am. Chem. Soc*., 2010, **132**, 8029; (*b*) M. Isik, R. Guliyev, S. Kolemen, Y. Altay, B. Senturk, T. Tekinay and E. U. Akkaya, *Org. Lett*., 2014, **16**, 3260; (*c*) M. Isik, T. Ozdemir, I. S. Turan, S. Kolemen and E. U. Akkaya, *Org. Lett*., 2013, **15**, 216.

10 M. Lan, J. Wu, W. Liu, H. Zhang, W. Zhang, X. Zhuang, P. Wang, *Sensor Actuat. B-Chem*., 2011, **156**, 332.

11 B. Liu, H. Tian. *Chem. Commu*., 2005, 3156.